Illustrating Deviations in the Beer–Lambert Law in an Instrumental Analysis Laboratory: Measuring Atmospheric Pollutants by Differential Optical Absorption Spectrometry

Heather C. Allen, Theo Brauers, and Barbara J. Finlayson-Pitts*
Department of Chemistry, University of California, Irvine, Irvine, CA 92697-2025

With the recent approval by the American Chemical Society of an undergraduate chemistry degree with an option in environmental chemistry, there is a need for relevant environmental experiments in the traditional chemistry core curriculum. We report here an experiment designed for an undergraduate junior/senior-level laboratory on instrumental analysis. It can be used to illustrate the basic components of a UV-vis absorption experiment, its application to the measurement of a number of atmospheric gases of interest, and the importance of understanding the conditions under which deviations from the simplest form of the Beer–Lambert law occur.

A wide variety of gases in both polluted and remote areas play a key role in the chemistry and radiative properties of the atmosphere (*1*). These include O_3, a toxic air pollutant for which the current air quality standard in the U.S. is 0.12 ppm for 1 hour (*2*). O_3 is also a greenhouse gas (*3*, *4*). It is the absorption of UV light by O_3 in the stratosphere that is responsible for the wavelength cutoff of light at the earth's surface at $\lambda \sim 290$ nm.

Other gases such as nitrogen oxides—NO_x ($NO + NO_2$)—are also inextricably linked to the formation and fate of O_3 (*1*). NO_2 is formed via oxidation of NO, directly emitted by combustion sources, by hydroperoxy or alkylperoxy free radicals:

$$NO + HO_2\,(\text{or } RO_2) \rightarrow NO_2 + OH\,(\text{or } RO) \qquad (1)$$

This leads to ozone formation by photolysis of NO_2:

$$NO_2 + h\nu \rightarrow NO + O(^3P) \qquad (2)$$

$$O(^3P) + O_2 \xrightarrow{M} O_3 \qquad (3)$$

Reactions 2 and 3 represent the sole known significant anthropogenic source of ozone in the troposphere. In areas with elevated NO_x levels such as continental sites, this source dominates other sources such as transport from the stratosphere.

Differential Optical Absorption Spectrometry (DOAS)

Owing to the complex mixture of gases present even in remote atmospheres, there is a critical need for sensitive and specific measurement techniques such as spectroscopic methods. While infrared absorption spectrometry has been applied to measure species such as O_3, HNO_3, and HCHO (*1*), the sensitivity is generally adequate only for the higher concentrations found in polluted urban areas. Application of UV-vis absorption spectrometry with its large absorption coefficients (i.e., cross sections) has the promise of higher sensitivity. The disadvantage of UV-vis absorption spectrometry applied to atmospheric measurements is that relatively few molecules have a "fingerprint" absorption spectrum with several unique bands, a requirement for selectivity. However, some key species in atmospheric chemistry, such as NO_2, O_3, SO_2, HCHO, naphthalene, HONO, and a variety of free radicals including NO_3, OH, and BrO do have structured absorptions and hence can be measured using this technique (*5*, *6*).

Another problem is the presence of many gases and particles that have broad and structureless absorptions in the UV/vis region, and that also cause light scattering. Thus it is not possible to measure the true, unattenuated light intensity (I_o) in the absence of light absorption, which is normally used in calculating absorbance in the laboratory. To overcome this problem, the technique of differential optical absorption spectrometry (DOAS) was developed (*5*, *6*). This method involves comparing the light intensity at a wavelength where the molecule of interest has a characteristic absorption band to that on either side of the known absorption. The latter is used as a measure of the light intensity in the absence of the absorbing species (I_o'), rather than the "true" value of I_o used in conventional laboratory experiments. The difference between I_o' and I_o is illustrated in Figure 1. For atmospheric applications of DOAS, it is also necessary to scan the spectral region of interest sufficiently fast that it is not affected by atmospheric turbulence. While the first DOAS systems (*5*) accomplished this using a unique rapid scanning mechanism and conventional photomultiplier, many recent studies employ a photodiode array detector.

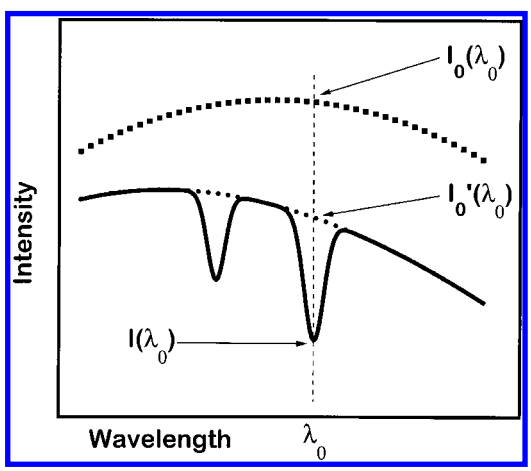

Figure 1. Conventional and differential absorption of an absorption band at the wavelength λ_0. The absolute absorption and differential optical densities are calculated as $D = \ln[I_0(\lambda_0)/I(\lambda_0)]$ and $D' = \ln[I'_0(\lambda_0)/I(\lambda_0)]$, respectively.

*Corresponding author: email *BJFINLAY@UCI.EDU*; phone 714/824-7670; fax 714/824-3168.

The Beer–Lambert Law and the Assumption of Monochromatic Radiation

The conventional form of the Beer–Lambert Law commonly applied to atmospheric gases is:

$$\ln \frac{I_o}{I} = \sigma N l \qquad (4)$$

where l is the path length, σ is the absorption cross section of the gas (cm^2/molecule), and N is the concentration (molecules cm^{-3}). It should be noted that in the atmospheric chemistry literature, absorption cross sections are normally reported using the natural log, ln, as in eq 4, rather than $\log_{10}$ as absorbance [$A = \log (I_o/I)$] is normally defined and measured by commercial spectrometers.

As discussed elsewhere (*7*, *8*), eq 4 applies to monochromatic radiation, or equivalently, to the situation where the absorption cross section is constant over the wavelength interval. One of the most common causes of nonlinearity in the Beer–Lambert law is the use of inadequate spectrometer resolution. In this case, the absorption cross section changes significantly over the spectral bandwidth used and plots of absorbance vs. concentration are nonlinear.

Recognition of the effects of inadequate resolution are becoming particularly important as manufacturers increasingly package instruments as computer-interfaced "black boxes", sometimes with libraries of absorption spectra to use for the determination of concentrations. If a user is not cognizant of the importance of defining the spectral resolution and understanding its effects on the Beer–Lambert law, large analytical errors can result from the application of a "calibration spectrum" taken at a different resolution. In addition, it is important to realize that the chemical composition may differ from samples used in the calibrations, owing to changes in equilibria etc.

Purposes of This Experiment

The experiment described here illustrates the following: (i) application of DOAS and the conventional Beer–Lambert law to the determination of an unknown NO_2 concentration in a gas cell; (ii) deviations from the Beer–Lambert law due to changes in the NO_2–N_2O_4 equilibrium and to changes in instrument resolution; (iii) the fundamental parameters that need to be measured to calculate absorbance (rather than relying on absorbance values provided directly by the instrument); (iv) the individual components of a typical UV/vis spectrometer and their functions; (v) typical monochromator calibration techniques.

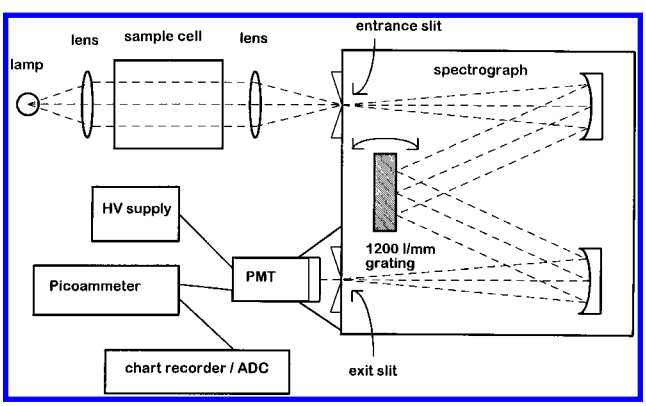

Figure 2. Experimental apparatus.

Experimental Apparatus

Figure 2 is a schematic diagram of the experimental apparatus. It consists of a white-light source (the lamp in a 35 mm projector was used here), lenses to focus the light on the entrance slit of a scanning monochromator, and a photomultiplier mounted on a flange at the exit slit. The signal from the photomultiplier is fed into a picoammeter and the output is recorded using a conventional strip-chart recorder or, alternatively, an analog-to-digital converter and computer. A low-pressure mercury lamp is used for wavelength calibration of the monochromator; as described below, this also provides an excellent illustration of how gratings function and the presence of higher orders at the exit slit. Finally, a series of gas cells of the same length (10–30 cm) containing known concentrations of NO_2 and one cell designated as the "unknown" are needed. These can be filled at the beginning of the course and used repeatedly throughout the quarter or semester.

Experimental Procedure

Calibration of Monochromator Using a Low-Pressure Mercury Lamp

The output of the low-pressure mercury arc (mounted in a housing to minimize exposure to UV) is first scanned to calibrate the monochromator. Figure 3 shows a typical scan with the mercury emission lines clearly marked. Note also the strong second-order line from the strongest 253.65 nm emission, which is observable if quartz optics are used. The second-order nature of this line can easily be demonstrated by placing a glass filter, which absorbs 253.65 nm, in the light path. This emission provides a good illustration of the grating law, $n\lambda = d(\sin i + \sin r)$, where i is the angle of incidence, r is the angle of diffraction, d is the spacing between the grooves, and n is the order of the diffraction. Thus the first-order ($n = 1$) 253.65 nm line is clearly seen, as is a line at 507.3 nm, which corresponds to second order ($n = 2$, $\lambda = 507.3/2 = 253.65$ nm).

Comparing and plotting the monochromator readings of the recorded emission lines against the "true" emission wavelengths (404.7, 435.8 nm; second order 253.65 nm at 507.3, 546.1, 577.0, and 579.1 nm) of the mercury lamp allows one to obtain a calibration curve. Correlation of the recorded spectrum with the true emission lines is obtained by visually observing the colors associated with a measured wavelength by removing the photomultiplier and placing a piece of paper in front of the exit slit.

Emission of the White-Light Source: Determination of I_o

The emission spectrum of the white-light source is then scanned with the empty cell in place to provide I_o as a function of wavelength (Fig. 4A); the zero intensity for this and scan B is shown on the vertical axis as 0(A,B).

Absorption Spectrum of NO_2*: Determination of* I

The individual gas cells are placed between the light source and the entrance slit and scanned. Figure 4B–D shows NO_2 spectra taken with exit slit widths of 1000, 100, and 10 μm, respectively, corresponding to resolutions (full width half maximum, FWHM) of 1.8, 0.26, and 0.11 nm; the zero lines for spectra C and D are shown on the left axis as 0(C) and 0(D). From such spectra, both optical densities $D = \ln (I_o/I)$ and $D' = \ln (I_o'/I)$ are calculated at the same absorption band.

The inset in Figure 4 shows the dependence of the differential optical absorption, $D' = \ln(I_o'/I)$, on the exit-slit width for the 448-nm band. It changes slowly with slit width at the higher resolutions, then drops off rapidly as the slit

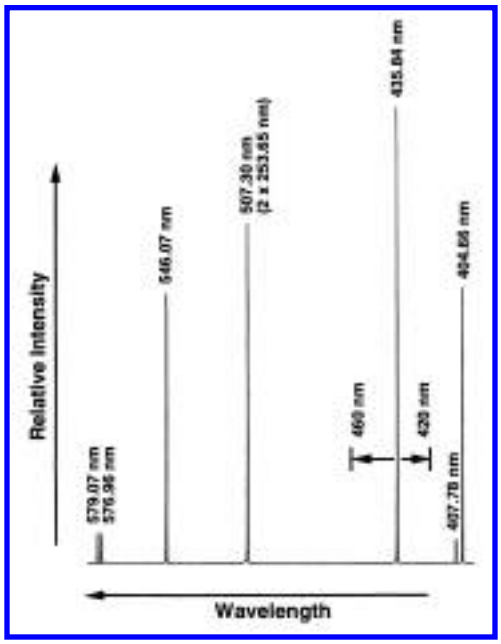

Figure 3. Spectrum of a mercury low-pressure lamp in the visible spectral region. The range between 420 and 460 nm was used for the absorption measurements.

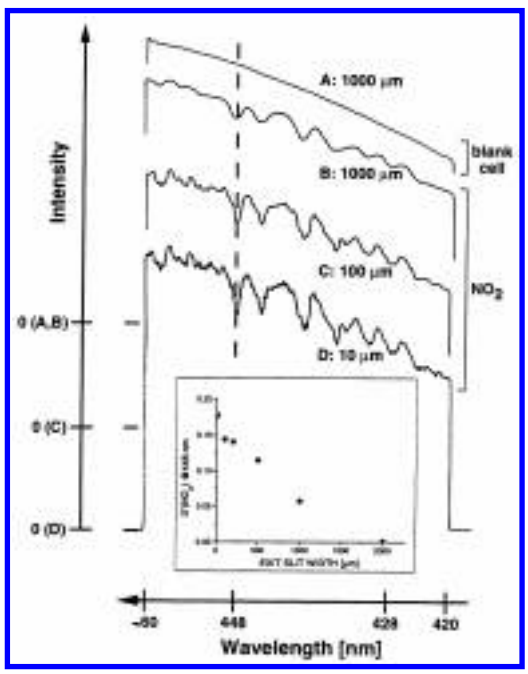

Figure 4. A: I_0 spectrum recorded using an empty cell. B, C, D: absorption spectra of NO_2 (2.5 torr) at different spectral resolutions. The spectra are displaced vertically for clarity and the zero intensity position for each of the spectra is shown on the left scale as 0(A,B), 0(C), and 0(D), respectively. Inset: Variation of the differential optical density D' at 448 nm (marked by the dashed line). Note that the differential absorption is invisible at the 2-mm exit slit width, corresponding to a 3.9-nm spectral resolution.

width increases. The optimum exit-slit width for these experiments is on the plateau, around 100 µm in this case. At higher resolutions, increased scatter occurs in the data due to previously unresolved rotational lines now becoming evident, as well as to increased noise at the lower light intensities. These factors are responsible for the discontinuity seen in the inset of Figure 4 at very small slit widths.

The data obtained in this experiment can be used to test two effects on the Beer–Lambert law: (i) a chemical effect, due to the NO_2–N_2O_4 equilibrium; and (ii) the effect of slit width or resolution. In the first case, the measured total pressures when NO_2 is placed in the cells have to be corrected for the equilibrium (*9*) with the dimer:

$$N_2O_4 \rightleftharpoons 2\ NO_2 \qquad K_p^{298} = 0.163 \qquad (5, -5)$$

The N_2O_4 dimer does not absorb light significantly at wavelengths longer than 400 nm (*10, 11*), so that corrections need only be made for the shift in the NO_2 concentration as a function of pressure, and not for any light absorption by the dimer.

As described in detail elsewhere (*12*), the equilibrium constant is related to the total measured pressure in the cell as given by:

$$K_p = \frac{4\alpha^2}{\left(1-\alpha^2\right)} \cdot \frac{P_{tot}}{P^\circ} \qquad (6)$$

where α is the fraction of N_2O_4 which dissociates, P_{tot} is the total measured pressure of NO_2 and N_2O_4, and P° is the standard state (1 bar and 298.15 K). Values of α are calculated at each measured total pressure and the pressure of NO_2 is then calculated from

$$P_{NO_2} = \frac{2\alpha}{\left(1+\alpha\right)} P_{tot} \qquad (7)$$

This correction is about 25% at the highest pressures used (~55 torr) in the 10-cm cell; use of a longer cell, e.g. 30 cm, would allow correspondingly smaller pressures to be used and hence smaller corrections for the N_2O_4.

Plots of the conventional absorbance, $\ln(I_0/I)$, and the differential optical absorbance, $\ln(I_0'/I)$, used in DOAS measurements, are shown as a function of the total measured pressure of (NO_2 + N_2O_4) (Fig. 5), and as a function of the NO_2 pressure corrected for the NO_2–N_2O_4 equilibrium (Fig. 6). Figure 5 clearly illustrates the nonlinearity of $\ln(I_0/I)$ and $\ln(I_0'/I)$ at higher NO_2 pressures where the relative concentration of NO_2 decreases due to the shift in the equilibrium towards the non-light-absorbing N_2O_4. Figure 6 shows that once the concentration data have been corrected for this shift in the equilibrium, nonlinearity can still clearly be seen at the larger slit widths (i.e., lower resolution), where the assumption of monochromatic radiation breaks down.

Use of Other Atmospherically Relevant Gases for This Experiment

NO_2 is a convenient gas of atmospheric importance to use for these experiments because it absorbs strongly in the visible region and is readily available from commercial gas suppliers. However, the experiment can also be applied to gases such as O_3 and SO_2. In this case, a light source such as a high-pressure Xe lamp is needed, requiring additional safety measures to avoid exposure to UV. Since the transmission of glass falls off rapidly towards 300 nm, it may also be necessary to use quartz windows. To study O_3, a means

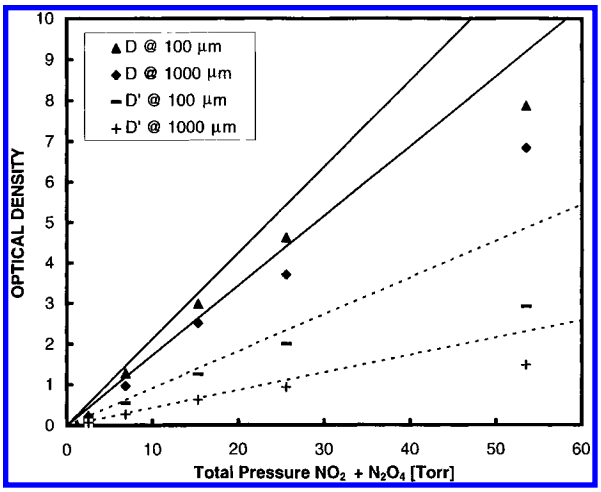

Figure 5. Optical densities (absolute and differential) at 2 spectral resolutions as a function of total pressure in the absorption cell. The lines are the least squares fits after correction for N_2O_4 (see Fig. 6) to show the influence of the N_2O_4 correction.

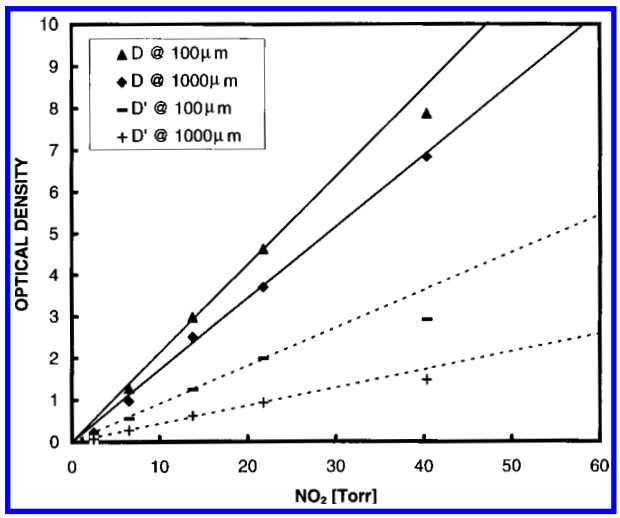

Figure 6. Optical densities as a function of NO_2 pressure calculated from eq 6. The lines represent least squares lines forced through the origin using the data points ≤ 22 torr of NO_2.

of generating this reactive gas is required, since it decays to O_2 on surfaces over time. Thus, unlike NO_2, the gas cells must be frequently pumped out and refilled for experiments that are carried out repetitively over a number of weeks.

While NO_2 is a convenient gas to use for these experiments, some photolysis can occur over time—particularly if quartz cells, which transmit in the UV, are used. In this case, reaction 2 followed by the reaction of $O(^3P)$ with NO_2 to form NO can lead to decreased NO_2 concentrations in the cell with time. Hence the cells should preferably be made of glass, kept in the dark when not in use, and recharged periodically with fresh NO_2.

Acknowledgments

We are grateful to Ara Apkarian, Peter Rentzepis, and Kenneth Janda for the loan of equipment in the initial development of this experiment, Sarka Langer for experimental assistance, John Hemminger and James N. Pitts, Jr., for helpful discussions, and the Camille and Henry Dreyfus Foundation for support of curriculum development of which this is a part.

Literature Cited

1. Finlayson-Pitts, B. J.; Pitts, J. N., Jr. *Atmospheric Chemistry: Fundamentals and Experimental Techniques*; Wiley: New York, 1986.
2. Cochran, L. S.; Pielke, R. A.; Kovács, E. *J. Air Waste Manage. Assoc.* **1992,** *42*, 1567–1572. (Note that this air quality standard is being revised to 0.08 ppm for 8 h.)
3. Ramanathan, V. *Science* **1988,** *240*, 293–299.
4. Rodhe, H. *Science* **1990,** *248*, 1217–1219.
5. Platt, U.; Perner, D.; Patz, H. W. *J. Geophys. Res.* **1979,** *84*, 6329–6335.
6. Platt, U. In *Air Monitoring by Spectroscopic Techniques, Chemical Analysis*, Vol. 127; Sigrist, M. W., Ed.; Wiley: New York, 1994, pp 27–84.
7. See for example, Wentworth, W. E. *J. Chem. Educ.* **1966,** *43*, 262–264.
8. Skoog, D. A.; Leary, J. J. *Principles of Instrumental Analysis*, 4th ed.; Saunders: Fort Worth, 1992; pp 127–131.
9. DeMore, W. B.; Sander, S. P.; Golden, D. M.; Hampson, R. F.; Kurylo, M. J.; Howard, C. J.; Ravishankara, A. R.; Kolb, C. E.; Molina, M. J. *Chemical Kinetics and Photochemical Data for Use in Stratospheric Modeling, Evaluation No. 11*; JPL Publ. No. 94-26, December 15, 1994.
10. Hall, T. C., Jr.; Blacet, F. E. *J. Chem. Phys.* **1952,** *20*, 1745–1749.
11. Calvert, J. G.; Pitts, J. N., Jr. *Photochemistry*, Wiley: New York, 1966.
12. Roscoe, H. K.; Hind, A. K. *J. Atmos. Chem.* **1993,** *16*, 257–276.